

Molecular analysis of *NOZZLE*, a gene involved in pattern formation and early sporogenesis during sex organ development in *Arabidopsis thaliana*

(anther/organogenesis/ovule)

URSULA SCHIEFTHALER[†], SURESHKUMAR BALASUBRAMANIAN[†], PATRICK SIEBER[†], DAVID CHEVALIER[†], ELLEN WISMAN[‡], AND KAY SCHNEITZ^{†§}

[†]Institute of Plant Biology, University of Zürich, Zollikerstr. 107, CH-8008 Zürich, Switzerland; and [‡]Max-Planck-Institut für Züchtungsforschung, Carl-von-Linné-Weg 10, D-50829 Cologne, Germany

Communicated by Elliot M. Meyerowitz, California Institute of Technology, Pasadena, CA, July 26, 1999 (received for review June 3, 1999)

ABSTRACT Sexual reproduction is a salient aspect of plants, and elaborate structures, such as the flowers of angiosperms, have evolved that aid in this process. Within the flower the corresponding sex organs, the anther and the ovule, form the male and female sporangia, the pollen sac and the nucellus, respectively. However, despite their central role for sexual reproduction little is known about the mechanisms that control the establishment of these important structures. Here we present the identification and molecular characterization of the *NOZZLE* (*NZZ*) gene in the flowering plant *Arabidopsis thaliana*. In several *nzz* mutants the nucellus and the pollen sac fail to form. It indicates that *NZZ* plays an early and central role in the development of both types of sporangia and that the mechanisms controlling these processes share a crucial factor. In addition, *NZZ* may have an early function during male and female sporogenesis as well. The evolutionary aspects of these findings are discussed. *NZZ* encodes a putative protein of unknown function. However, based on sequence analysis we speculate that *NZZ* is a nuclear protein and possibly a transcription factor.

The elucidation of the molecular mechanisms underlying organogenesis continues to represent a formidable challenge for biologists. In this context the plant reproductive organs recently have attracted considerable attention. The life cycle of plants alternates between the diploid sporophytic and the haploid gametophytic phase. The sporophyte produces the unisexual spores that produce the gametophyte, which in turn develops the gametes (1). Upon fusion of the gametes a new sporophyte comes into existence. In angiosperms these essential processes occur within the principal male and female sex organs of the plant: the anther and the ovule.

What is their general structure? The ovule is the progenitor of the seed and as such a more elaborate structure than the anther. In a typical ovule usually three major elements can be recognized (2). At the distal end the nucellus constitutes the female spore-bearing tissue or megasporangium. During sporogenesis the megaspore mother cell (MMC) undergoes meiosis and forms a tetrad of megaspores. Only one of the megaspores continues gametophytic development, eventually giving rise to an embryo sac with the egg cell proper. Centrally the chalaza is characterized by usually two integuments that initiate at its flanks. The integuments will encapsulate the nucellus and the developing embryo sac except for a small cleft, the micropyle, through which the pollen tube grows during the fertilization process. After fertilization they develop into the seed coat. The funiculus is the stalk that connects the ovule to

the carpel. On the male side the pollen sac or theca represents the microsporangium (2). Usually two pairs of thecae are present per anther and separated by vasculated sterile tissue. A periclinal division in several adjacent hypodermal cells, the archesporia, at four corners of the anther primordium initially characterizes the development of the pollen sacs, which leads to the inner primary sporogoneous cells and the outer primary parietal cells. The sporogoneous cells may divide further but they often develop directly into the pollen mother cells (PMCs). The parietal cell layer undergoes additional divisions and eventually the endothecium, the middle layer and the tapetum, which is located next to the developing PMCs, are formed. The PMCs proceed with meiosis, which will result in tetrads of microspores. Those microspores develop into the mature pollen grains containing the male gametophyte with the sperm cells.

The ovule, in particular of *Arabidopsis thaliana*, has become an excellent model system to study organogenesis. Through the efforts of a number of labs a framework of ovule development currently is evolving. A large number of genes with a role in ovule development have been identified, and those loci are being characterized at the genetic and molecular level (for recent reviews see refs. 3 and 4). One prominent question deals with pattern formation. For example, how are the three elements, the nucellus, chalaza, and funiculus, set up? There is a lot of indirect evidence that supports a corresponding early subdivision of the ovule primordium (4, 5); however, only one candidate is known that may be directly involved in establishing one of these elements. Mutations in the *BELL* (*BEL1*) gene lead to an altered chalazal development and outgrowths of unknown identity develop in place of integuments (6–8). The *BEL1* locus encodes a homeodomain putative transcription factor and its RNA expression pattern becomes restricted to the central region before the initiation of the integuments (9).

In this context a number of important questions surface. For example, what genes regulate the formation of the nucellus and are they related to *BEL1*? Does the formation of the nucellus and pollen sac, two quite different sporangia, involve common factors? As a first step toward the elucidation of these questions we describe in this paper the identification and molecular characterization of the *NOZZLE* (*NZZ*) gene in *A. thaliana*. The *NZZ* locus encodes a novel protein. The *nzz* mutant phenotype indicates that *NZZ* has a role in the establishment of the pollen sac and nucellus and possibly an early role in sporogenesis.

Abbreviations: MCC, megaspore mother cell; PMC, pollen mother cell; RT-PCR, reverse transcription-PCR.

Data deposition: The sequence reported in this paper has been deposited in the GenBank database (accession no. AF146794).

[§]To whom reprint requests should be addressed. E-mail: Kay.Schneitz@access.unizh.ch.

The publication costs of this article were defrayed in part by page charge payment. This article must therefore be hereby marked "advertisement" in accordance with 18 U.S.C. §1734 solely to indicate this fact.

PNAS is available online at www.pnas.org.

METHODS

Plant Work and Genetics. Plants were grown as described (8), and *A. thaliana* (L.) Heynh. var. Landsberg (*erecta* mutant) was used as the wild-type strain. The *nzz-1* and *nzz-3* mutants were found in an *En-1/Spm*-transposon-induced mutant population (Columbia ecotype) (10) whereas the *nzz-2* mutant was isolated in a screen by using ethyl methane sulfonate as mutagen (*Ler* ecotype). The mutations were shown to be allelic (not shown). The *nzz-1* and the *nzz-2* alleles were used in two independent mapping experiments involving outcrosses to *Ler* and Columbia plants, respectively. The combined results yielded a map position between markers PG11 (2/130 recombinant chromosomes) and PRHA (7/132) on chromosome 4.

Molecular Identification of *nzz* Mutations. Genomic DNA flanking the left side of the *En-1* insertions in *nzz-1* (after outcrossing to reduce the *En-1* copy number) was isolated by PCR using nested *En-1*-specific and splinkerette-based primers (11) and subcloned into the vector pCR 2.1 (Invitrogen). The *En-1*-specific primers were En-225 (CACGACGGCTGTAGAATAGGATTGGGGAATTT) and En-93 (GGTGCA-GCAAACCCACACTTTTACTTCGATTAAG). Genomic clones from the right side of the *En-1* insertion were obtained by using a second set of primers based on the sequence of clone ATM4I22.140. They were: for *nzz-1*, *En-1*-specific CGGAA-TTCGAGTGTGCGTTGCTTGTTGAA and *NZZ*-specific CCAAAGGGTAATCCAAAGC; for *nzz-3*, *En-1*-specific TCAGGCTCACATCATGCTAGTCC (En-7631) and *NZZ*-specific GAATCATGACAGGATCATTGC. Genomic clones from the left side of *nzz-3* were isolated by using a third set of primers: *En-1*-specific, AGCACGACGGCTGTAGAATAG-GATTG (En-203); *NZZ*-specific, CATCGATCTTAACA-ACGCT. The footprint allele *nzz-1** was confirmed by sequencing three independent copies of PCR fragment subclones generated by using *nzz-1** genomic DNA and two primers flanking the *En-1* insertion site in the *nzz-1* mutant (AGGACTGCAATCACCTACGAG, GTGACACTTGCTT-CAAGTTT). To identify the *nzz-2* mutation a *nzz-2* genomic DNA fragment was amplified by PCR and subcloned, and three different clones were sequenced. An identical approach was used to generate the *Ler* wild-type sequence. The ATM4I22 sequence (AL030978) and the *Ler* genomic sequence of *NZZ* (AF146794) can be found in the GenBank database.

DNA Work and cDNA Isolation. Regular protocols were used for routine DNA work (12). Several cDNA clones were obtained through a 5' and 3' rapid amplification of cDNA ends (RACE) approach (13) by using the Marathon kit (CLONTECH) and poly(A)+ RNA from flowers of stages 1–12 (14) (Columbia ecotype). The following nested *NZZ*-specific primers were used: CTGATCGTAGCCGTTTCATCGGAGGAGG and GTGTATTTTCGAAAATCCACCACCGTTGG (5' RACE) as well as GATCTCTAACAACGCTACCCGTTT-ACCC and GTGTTGTGCTACAAGGCTTCCCAAGC (3' RACE). The longest PCR fragments were sequenced on both strands. Sequences were obtained by standard cycle sequencing using an ABI 373 sequencer (Applied Biosystems).

RNA Work and Reverse Transcription-PCR (RT-PCR). Total RNA was isolated from inflorescences (12) carrying flowers from stage 1 to 12. The poly(A)+ RNA was isolated by using oligo(dT)25-Dynabeads according to the manufacturer's protocol (Dyna). For Northern analysis 10 μ g of poly(A)+ RNA was loaded on a formaldehyde-agarose gel. After electrophoresis the poly(A)+ RNA was blotted onto a Hybond-N nylon membrane (Amersham Pharmacia) and hybridized according to the manufacturer's recommendations. The RNA size marker G319 was included for size calibration (Promega). A genomic DNA PCR fragment spanning the 3' two-thirds of the gene (nucleotides 58168–59191, see Fig. 2) was labeled with [α -³²P]dCTP (3,000 Ci/mmol) and used as

probe. Exposure was for 4 days at -80°C by using a Kodak Biomax MS film with the help of an intensifying screen. For the RT-PCR experiments 2 μ g of poly(A)+ RNA, isolated from the corresponding tissue, was reverse-transcribed with Moloney murine leukemia virus reverse transcriptase (NEB, Beverly, MA). The following *NZZ*-specific primers, flanking the first intron, were used for PCR: AGTACTAGAAGCAGAA-ACTGAAGCTG and CATCGATCTCTAACAACGCT. The PCR products were loaded on an agarose gel and a Southern blot analysis was performed. The same probe as in the Northern experiment was used. As a control a RT-PCR using primers corresponding to the *Arabidopsis GAPC* gene (15) (CTGTTGTGCGCAACGAAGTC, CACTTGAAGG-TGGTGCCAAG) was performed.

In Situ Hybridization. Digoxigenin-based (DIG) nonradioactive *in situ* hybridization experiments using 8- μ m sections of paraffin-embedded material were carried out essentially as described (16). An about 1.5-kb genomic DNA PCR fragment, spanning most of the transcribed region (nucleotides 58169–59657, see Fig. 2), was subcloned into the pCR II-TOPO vector (Invitrogen). To generate antisense and sense RNA probes the subclone was linearized with *Xba*I and *Bam*HI, respectively, and *in vitro* transcribed (including DIG-UTP, Roche Diagnostics) by using SP6 (Roche Diagnostics) or T7 RNA polymerase (NEB) as described (17).

Ovule Preparations, Microscopy, and Artwork. Light microscopy, scanning electron microscopy, staging, whole-mount ovule preparations, and artwork have been described (5, 8, 17). Whole-mount anthers were prepared in exactly the same way as whole-mount ovules.

RESULTS

The *nzz* Mutant Phenotype. A summary of the visible defects that occur in *nzz* mutants is given in Fig. 1. A detailed genetic analysis of *NZZ* will be presented elsewhere (S.B. and K.S., unpublished work). The wild-type development of ovules and anthers in *Arabidopsis* has been described by several authors (5–7, 18–20). In *nzz* mutants alterations apparently are restricted to the anthers and ovules. Very early defects in the development of both organs can be observed. In the ovule the distal tip tissue (normally the nucellus) usually is very much reduced, sometimes even appears absent, and a MMC usually is not detected. As a result no nucellus and no embryo sac can be seen at later stages. Furthermore, the inner integument initiation is delayed and the integuments often are reduced, in some instances they are missing (not shown), and the funiculus is longer because of a higher cell number (not shown). In the young anther the initial periclinal division of the archesporial cells that leads to the primary parietal layer and the PMCs cannot be observed. Only a mass of subepidermal uniform cells is apparent throughout development and at late stages no pollen sacs are seen. As a result of those defects *nzz* mutants are male and female sterile.

Molecular Identification of the *NZZ* Gene. We have isolated three independent mutant alleles of *NZZ*, two of which were obtained by using an *En-1* transposon-tagging approach (see *Methods*). The frequent presence of fertile revertant sectors in *nzz-1* mutants (not shown) indicated that the *NZZ* locus was tagged. Genomic DNA flanking the left side of the *En-1* insertion sites in *nzz-1* mutants was isolated and sequenced. Sequence database searches showed one of the sequences obtained to be identical to a sequence corresponding to clone ATM4I22.140. This clone stems from the *Arabidopsis* genome project, corresponds to a gene-coding region, and maps to the same interval on chromosome 4 as *NZZ*. The sequence information from this clone was used to design PCR primers that were successfully used to clone the right flanking region of *nzz-1*, to identify and clone the genomic DNA of the *En-1* insertion site of *nzz-3*, and to identify a point mutation in this

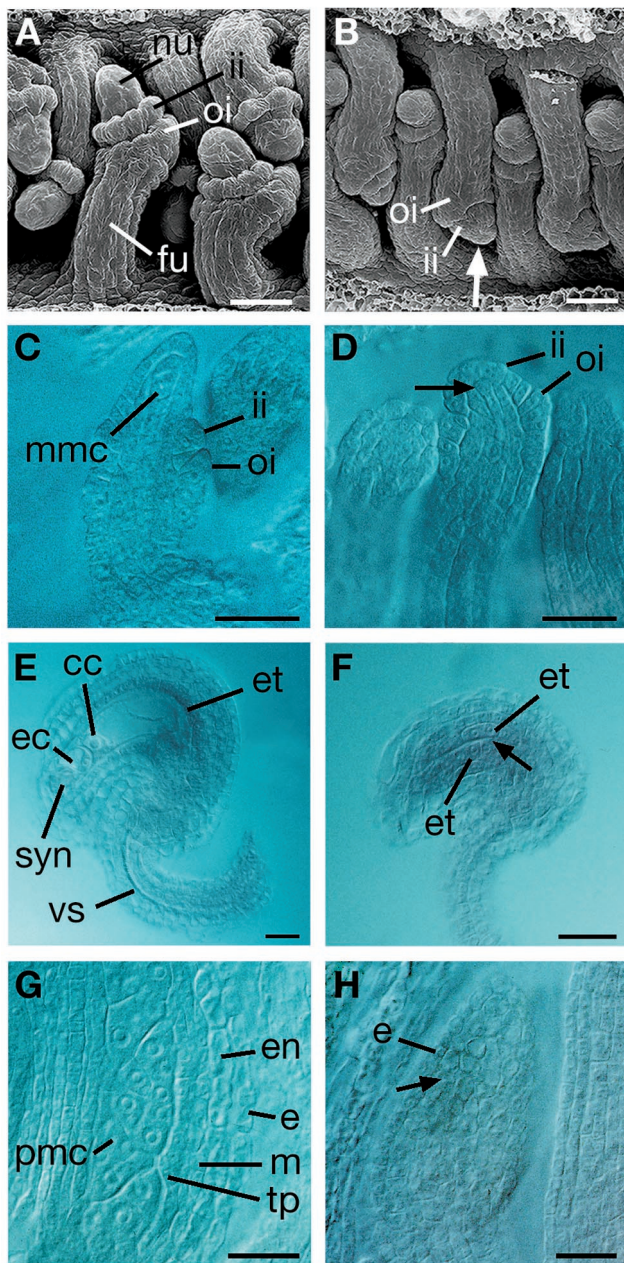


FIG. 1. Summary of the *nzz* mutant phenotypes. (A and B) Scanning electron micrographs. (C–H). Optical sections through whole-mount tissue. (A, C, E, and G) Wild type. (B, F, and H) *nzz-2*. (D) *nzz-1*. Stages: (A–D) ovule stage 2–III, (E and F) ovule stage 3–VI, (G and H) floral stage 7. (A and C) The nucellus is prominent and the two integuments are initiated. (B and D) Note the reduced distal tip region (arrow) and compare with A and C. (E) A fully developed embryo sac and fully developed integuments are seen. (F) There is a prominent absence of a nucellus and an embryo sac at this stage (arrow). The integuments are reduced; however, an endothelium still can be recognized. (G) An anther at a premeiotic stage. The PMCs and the descendants of the primary parietal layer are clearly recognizable. (H) Only a mass of uniform cells is detectable in this anther (arrow). cc, central cell; e, epidermis; ec, egg cell; en, endothecium; et, endothelium; fu, funiculus; ii, inner integument; m, middle layer; mmc, megaspore mother cell; nu, nucellus; oi, outer integument; pmc, pollen mother cell; syn, synergid; tp, tapetum; vs, vascular strand. (Scale bars, 20 μ m.)

region in *nzz-2* (Fig. 2 A and B) (see *Methods*). During the process of identifying the *En-1* insertion that causes the *nzz* mutant phenotype in *nzz-1* mutants on a Southern blot, using genomic DNA derived from members of a segregating popu-

lation, a mutant plant carrying a putative footprint mutation (*nzz-1**) was identified (not shown). The footprint mutation was expected to have arisen because of the imprecise excision of the *En-1* transposon. This possibility was verified by sequence analysis of the *nzz-1** DNA spanning the corresponding *En-1* insertion site. The result showed that a 2-bp insertion is present in the *nzz-1** mutant (Fig. 2B).

Molecular Characterization of NZZ. The longest cDNA spans a region of 1.285 kb (Fig. 2A), a value in good agreement with the 1.4-kb transcript length as shown by Northern analysis (see Fig. 4A). There is an at least 88-bp 5' and a 252-bp 3' untranslated region and there are two small introns of 99 bp and 89 bp, respectively. The longest ORF, after conceptual translation, encodes a 314-aa protein with a calculated molecular mass of 31.1 kDa. The putative NZZ protein sequence does not show any significant homology to entries in the European Molecular Biology Laboratory/GenBank sequence databases. However, close examination of the protein sequence by computer analysis revealed several features (Figs. 2 and 3).

Overall the protein appears to be hydrophilic (Fig. 3). In particular there is an about 40-residue domain, which we call PC domain for polar-charged domain, spanning residues 41–80 with 22.5% polar residues and 45% charged residues (35% basic and 10% acidic aa). A hydropathicity blot (21) revealed three somewhat less hydrophilic regions. There is a larger, so-called middle region, which includes residues 81–146 and contains 39.4% hydrophobic residues. In addition, there may exist two smaller regions, separated by 40 aa, which span residues 232–247 (D1) and 288–302 (D2). Scanning the PROSITE database (22) for protein domain signatures revealed imperfect matches of the D1 and D2 sequences with the signature for a myc-type helix-loop-helix (HLH) protein dimerization domain (but see *Discussion*). In addition, one can find two candidate nuclear localization signals (23) (Fig. 2A). A number of potential amidation, glycosylation, myristylation, and phosphorylation signals are present in the putative NZZ protein sequence (not shown), which could indicate that the NZZ protein undergoes posttranslational modifications.

All three *nzz* mutations map within the transcribed region of NZZ (Fig. 2). In the case of *nzz-1* the *En-1* insertion is just after nucleotide 58638. In this mutant a partially truncated protein of 254 residues still could be formed (with the last 10 residues being encoded by the left end of the *En-1* element; not shown). Such a protein would carry an aberrant D1 part and lack the remainder, including the D2 region, of the wild-type NZZ protein. In *nzz-2* mutants a G to A transition at nucleotide 59040 results in a stop codon. Thus, a protein of 142 residues could be produced that lacks a putative nuclear localization signal and the D1 and D2 region. The *nzz-3* mutation is caused by an *En-1* insertion just after nucleotide 58315 in the 3' untranslated region. Thus, it raises the possibility for a role of this region in for example mRNA stability or translational control of NZZ (24).

The Temporal and Spatial Expression Pattern of NZZ Transcripts. As expected from the spatial extent of the *nzz* mutant phenotype (Fig. 1) NZZ transcripts are found in flowers (Fig. 4A). Interestingly, transcripts also are detected in rosette leaves, stem tissue, and seedlings (Fig. 4B). To investigate the spatial and temporal localization of NZZ transcripts during floral development a series of *in situ* hybridization experiments were performed (Fig. 5). Here we will focus on the expression of NZZ during early anther and ovule development. However, NZZ transcripts can be detected in petals, carpels, and nectaries, and weak staining also is seen in the vascular tissue of the inflorescence (not shown).

With respect to ovule development NZZ expression is seen during all of stage I and throughout the ovule primordium (Fig. 5 A and B). At stage 2-I the MMC also is staining. During stages 2-II/III, when the two integuments initiate, NZZ is

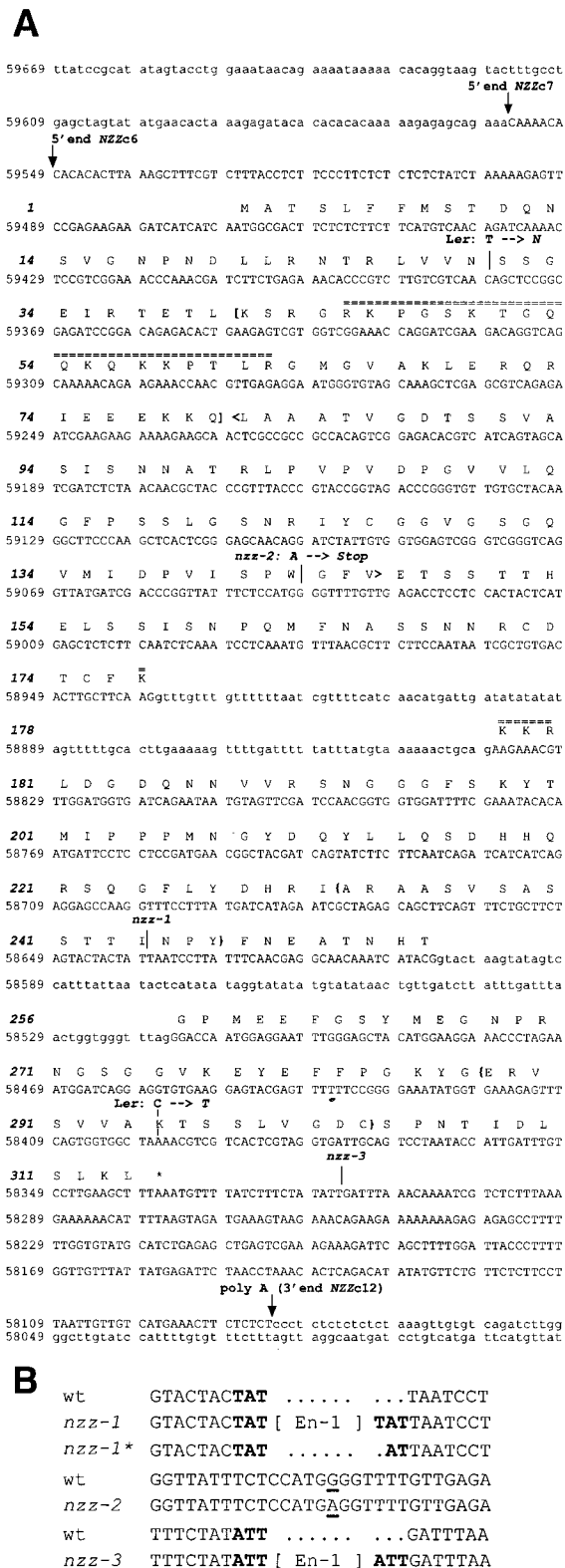


FIG. 2. Sequence analysis of the *NZZ* gene. (A) The genomic DNA sequence of the *NZZ* gene [between 113 bp upstream of the longest cDNA (*NZZc7*) and 94 bp downstream of the poly(A) addition site] and the corresponding amino acid sequence of the putative *NZZ* protein are shown. Uppercase letters represent exon sequences. The 5' end of *NZZ* points to the southern telomer. The numbering of nucleotides corresponds to the numbering given in the sequence of clone ATM4122. The numbering of the amino acids is indicated by bold and italic letters. The sequence corresponds to the Columbia ecotype. There are two nucleotide sequence polymorphisms in *Ler*, at positions 58397 and 59379. Both changes and the corresponding amino acids are

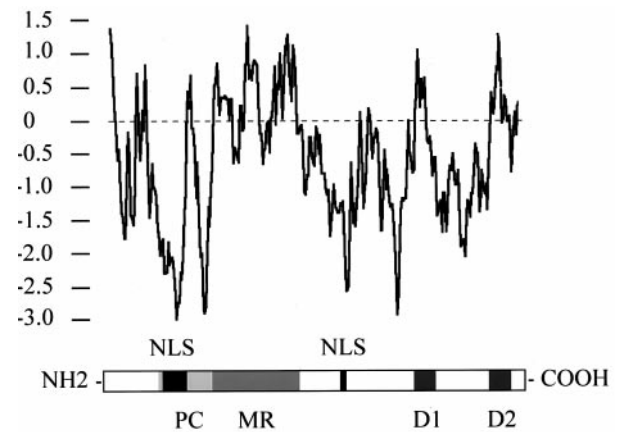


FIG. 3. Aspects of the putative *NZZ* protein. (Upper) A hydrophobicity plot (21) is given. (Lower) A corresponding scheme details the hypothetical regionalization.

somewhat stronger expressed in both developing integuments (Fig. 5C) whereas weak expression throughout the ovule is still apparent. During stage 3 prominent staining is visible in the proximal part of the endothelium (not shown).

The *NZZ* expression is visible throughout the anther primordium at early floral stage 7 and before the initial archesporial periclinal cell divisions (Fig. 5D). During further anther development *NZZ* continues to be broadly expressed with somewhat less stain visible in the epidermis (Fig. 5E). By the time of early meiosis *NZZ* transcripts apparently are restricted to the PMCs and the tapetum (Fig. 5F). The staining continues to be present in these two cell types until the pollen grains are released from the tetrads. After this stage *NZZ* expression can be detected only in individual pollen grains but quickly vanishes there as well (not shown).

The transcript patterns in other floral organs such as petals, carpels, and nectaries, as well as the expression found in rosette leaves, stem tissue, and seedlings, was unexpected as we could not detect a visible phenotype in these tissues. This finding can be explained in several ways. There is the possibility that *NZZ* may have no function in these parts of the plant or that the defects cannot easily be detected. One also could imagine that in these tissues the absence of *NZZ* activity in *nzz* mutants is compensated for by additional redundant factors.

DISCUSSION

Here we report our results on the molecular characterization of *NOZZLE*. The cloning of the *NZZ* locus was achieved by a transposon-tagging approach. We have molecularly characterized three independent *nzz* alleles. All the mutations map within the same gene, within exons, and two are located in the protein-coding part of the gene. Taken together, these data show that we have cloned and identified the *NZZ* locus.

indicated above the sequence. The former alteration leads to an amino acid change. The positions of the three *nzz* mutations and the 5' and 3' ends of *NZZ*-cDNAs also are indicated. At the amino acid level the charged and hydrophobic domains as well as the D1 and D2 domains are flanked by brackets and braces, respectively. Double lines above the sequence highlight the two putative nuclear localization motifs. (B) Identification of *NZZ*. Genomic sequences found in the *nzz-1*, *nzz-1**, *nzz-2*, and *nzz-3* mutants and flanking the individual mutations are given as are the corresponding wild-type sequences. *nzz-1** represents a mutant revertant of *nzz-1*. Bold letters refer to the target site duplications generated by the *En-1* transposons. In the case of the *nzz-1* and *nzz-3* mutations the orientation of the *En-1* elements is the same (left end to the left). Note the presence of a 2-bp footprint in *nzz-1**. The position of the G to A transition in *nzz-2* is underlined.

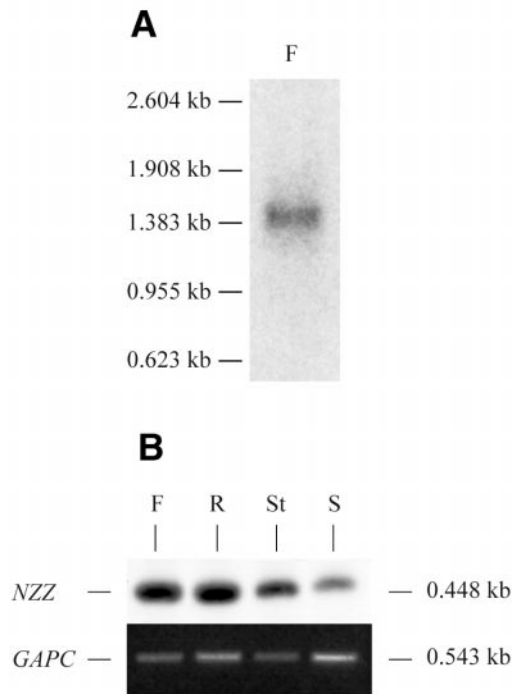


FIG. 4. The size and tissue distribution of *NZZ* transcripts. (A) Northern analysis. A single band of about 1.4 kb can be detected. (B) A RT-PCR/Southern experiment involving different tissues (see *Methods*). Expression can be detected in flowers, rosette leaves, stem tissue, and seedlings. (C) Control RT-PCR using the *Arabidopsis* *GAPC* gene. F, flowers from stages 1–12; R, rosette leaves; S, 8- to 10-day-old seedlings; St, stem.

The Biochemical Function of the Putative *NZZ* Protein. Because of the novel structure of *NZZ* the biochemical function of the *NZZ* protein at present remains obscure. The significance of the match of the D1 and D2 regions to the PROSITE myc-type helix-loop-helix (HLH) protein dimerization signature is unclear as well because no HLH protein sequences were pulled out in corresponding database searches. The myc-related HLH proteins represent a group of transcription factors that act as dimers (25). Nevertheless, a few hints prompt us to speculate that *NZZ* could be a transcription factor. There are two putative nuclear localization signals and the basic polar-charged region might bind DNA. The middle region stretch and the D1/D2 region could be involved in protein-protein interactions. The *nzz-1* and *nzz-2* (a strong allele) mutations indicate that the region is important for *NZZ* function. Obviously more data are required to address these questions.

The Role of *NZZ* During Anther and Ovule Development. The mutant phenotype and the expression pattern indicate that *NZZ* plays a wider role during ovule development as compared with anther ontogenesis. Here we focus on the requirements of *NZZ* for sporangium formation. The observed expression of *NZZ* in the chalaza, the integuments, and the funiculus is compatible with a function of *NZZ* in aspects of ovule ontogenesis other than nucellus development. They will be discussed in great detail in a separate paper (S.B. and K.S., unpublished work).

It seems reasonable to infer from these data that *NZZ* has equivalent functions during the early formation of the two types of sporangia, the nucellus and the pollen sac (see also below). What role could that be? The data are compatible with essentially two possibilities. One primary function of *NZZ* could reside in the establishment of the distal region of the ovule primordium and the equivalent regions in the young anther. In *nzz* mutants the reduction of the nucellus and pollen

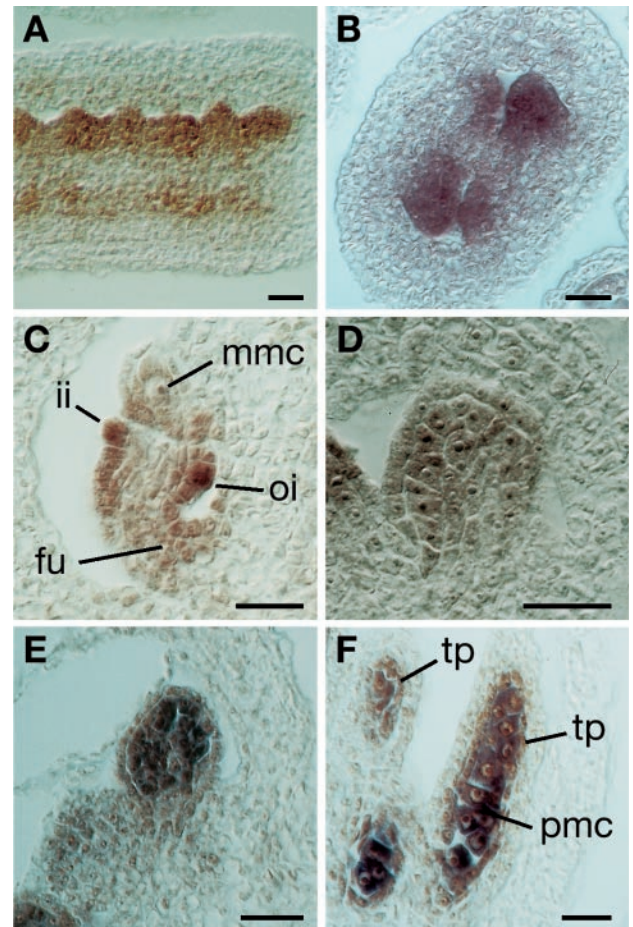


FIG. 5. The wild-type *NZZ* transcript pattern during early anther and ovule development as revealed by *in situ* hybridization on tissue sections. (A and F) Oblique longitudinal sections. (B–E) Longitudinal sections. (A) Young ovule primordia of stage 1. All the ovule tissue is staining. (B) An ovule at stage 1-II. Again the entire primordium is staining. (C) An ovule at stage 2-III. The labeling includes the MMC. In this section the posterior (abaxial) side of the inner integument is not visible. Note the stronger epidermal signal that can be detected in the developing integuments. (D) An anther primordium at early floral stage 7 before the archesporial periclinal divisions. The *NZZ* RNA is expressed throughout the primordium. (E) An anther slightly older than in D. Note the reduced staining in the epidermis (arrow). (F) An anther at an early meiotic stage. The *NZZ* expression is restricted to the PMCs and the surrounding tapetum. Control experiments using a sense probe gave no signals (not shown). ii, inner integument; fu, funiculus; mmc, megaspore mother cell; oi, outer integument; pmc, pollen mother cell; tp, tapetum. (Scale bars, 20 μ m.)

sacs are compatible with this explanation. Thus, the failure to form a MMC in ovules and the PMCs and parietal cell layers in anthers would be a secondary effect. The early broad transcript expression of *NZZ* in both types of primordia supports such a view as well. Alternatively, *NZZ* could have a primary role in establishing the sporogeneous lineage. In the absence of a functional MMC and the male archesporial nucellus and pollen sacs would fail to proceed in their proper development. If true this would indicate that cells of the sporogeneous lineage somehow influence the development of the sporangium through cell-cell communication. The expression of *NZZ* in the MMC and the PMCs corroborates this possibility. To us the former view appears as the most parsimonious explanation of our findings and thus we favor the view of *NZZ* being an important factor in establishing the distal, i.e., the prospective spore-producing region of the ovule and anther primordia. However, at present we cannot rule out that *NZZ*

also is required for a very early step of male and female sporogenesis.

The Evolution of Heterospory. The likelihood that *NZZ* has equivalent functions during the early establishment of the two types of sporangia possibly has implications with respect to questions that address the evolution of heterospory and heterosporangy. Higher plants exhibit heterospory, which is always coupled with heterosporangy (1). It is accepted that heterospory evolved from homospory, and that this process may have occurred several times independently during vascular plant evolution, including in the ancestor of the seed plants (26). However, little is known about the evolutionary transition between homospory and heterospory and the ontogenetic development of the latter. The analysis of *NZZ* provides genetic and molecular support for the view that the heterosporous seed plants evolved from a homosporous ancestor, and that *NZZ* orthologues may exist in homosporous basal vascular plants. Thus, the *NZZ* gene should provide an excellent tool to address these important questions in vascular plant evolution.

Note Added in Proof. While this work was in press, Yang *et al.* (27) reported the cloning and identification of the *NOZZLE* gene under the name of *SPOROCYTELESS*.

We thank Heinz Saedler and ZIGIA, Max-Planck-Institut für Züchtungsforschung, Cologne, for making available the *En-1*-induced mutant lines. We thank Peter Endress, Yin-Long Qiu, and Ulrike Utans Schneitz for helpful discussions and Röbi Dudler for comments on the manuscript. We also thank Antje Redweik for expert technical assistance and Jean-Jacques Pittet for the artwork. U.S. is the recipient of a postdoctoral fellowship from the Austrian Schrödingerstiftung. This work was funded by grants from the Swiss National Science Foundation (31-42175.94, 31-53032.97) to K.S. and by the Kanton of Zürich.

- Gifford, E. M. & Foster, A. S. (1989) *Morphology and Evolution of Vascular Plants* (Freeman, New York).
- Esau, K. (1977) *Anatomy of Seed Plants* (Wiley, New York).
- Gasser, C. S., Broadhvest, J. & Hauser, B. A. (1998) *Annu. Rev. Plant Physiol. Plant Mol. Biol.* **49**, 1–24.
- Schneitz, K. (1999) *Curr. Opin. Plant Biol.* **2**, 13–17.
- Schneitz, K., Hülskamp, M. & Pruitt, R. E. (1995) *Plant J.* **7**, 731–749.
- Robinson-Beers, K., Pruitt, R. E. & Gasser, C. S. (1992) *Plant Cell* **4**, 1237–1249.
- Modrusan, Z., Reiser, L., Feldmann, K. A., Fischer, R. L. & Haughn, G. W. (1994) *Plant Cell* **6**, 333–349.
- Schneitz, K., Hülskamp, M., Kopczak, S. D. & Pruitt, R. E. (1997) *Development (Cambridge, U.K.)* **124**, 1367–1376.
- Reiser, L., Modrusan, Z., L., M., Samach, A., Ohad, N., Haughn, G. W. & Fischer, R. L. (1995) *Cell* **83**, 735–742.
- Wisman, E., Hatmann, U., Sagasser, M., Baumann, E., Palme, K., Hahlbrock, K., Saedler, H. & Weisshaar, B. (1998) *Proc. Natl. Acad. Sci. USA* **95**, 12432–12437.
- Devon, R. S., Porteous, D. J. & Brookes, A. J. (1995) *Nucleic Acids Res.* **23**, 1644–1645.
- Sambrook, J., Fritsch, E. F. & Maniatis, T. (1989) *Molecular Cloning: A Laboratory Manual* (Cold Spring Harbor Lab. Press, Plainview, NY), 2nd Ed.
- Frohman, M. A., Dush, M. K. & Martin, G. R. (1988) *Proc. Natl. Acad. Sci. USA* **85**, 8998–9002.
- Smyth, D. R., Bowman, J. L. & Meyerowitz, E. M. (1990) *Plant Cell* **2**, 755–767.
- Shih, M. C., Heinrich, P. & Goodmann, H. M. (1991) *Gene* **104**, 133–138.
- Long, J. A., Moan, E. I., Medford, J. I. & Barton, M. K. (1996) *Nature (London)* **379**, 66–69.
- Schneitz, K., Baker, S. C., Gasser, C. S. & Redweik, A. (1998) *Development (Cambridge, U.K.)* **125**, 2555–2563.
- Bowman, J. (1994) *Arabidopsis: An Atlas of Morphology and Development* (Springer, New York).
- Misra, R. C. (1962) *Univ. J. Res. Agra* **11**, 191–199.
- Owen, H. A. & Makaroff, C. A. (1995) *Protoplasma* **185**, 7–21.
- Kyte, J. & Doolittle, R. F. (1982) *J. Mol. Biol.* **157**, 105–132.
- Bairoch, A., Bucher, P. & Hofmann, K. (1997) *Nucleic Acids Res.* **24**, 217–221.
- Dingwall, C. & Laskey, R. (1991) *Trends Biochem. Sci.* **16**, 478–481.
- Bailey-Serres, J. (1999) *Trends Plant Sci.* **4**, 142–148.
- Lüscher, B. & Eisenmann, R. N. (1990) *Genes Dev.* **4**, 2025–2035.
- Bateman, R. M. & DiMichele, W. A. (1994) *Biol. Rev.* **69**, 345–417.
- Yang, W.-C., Ye, D., Xu, J. & Venkatesan, S. (1999) *Genes Dev.* **13**, 2108–2117.